Identification of the Matrix Shift: A Fingerprint for Neutral Neon Complex?

Yuriko Taketsugu, Takeshi Noro, and Tetsuya Taketsugu*

Division of Chemistry, Graduate School of Science, Hokkaido University, Sapporo 060-0810, Japan

Received: November 12, 2007

Ar−NiCO and Ne−NiCO have been predicted as novel neutral noble gas charge-transfer complexes, with binding energies of 7.70 and 2.16 kcal/mol, respectively, by the highly correlated coupled-cluster singles and doubles including a perturbational estimate of triple excitations calculations. The calculated shifts in the Ni−C−O bending frequency are 48 and 36 cm^{-1} for Ar−NiCO and Ne−NiCO, while the corresponding experimental matrix shifts are 46 and 36 cm^{-1}, respectively. The anharmonicity effects for these frequencies are verified to be very small. The interaction between a noble gas atom and NiCO is discussed through natural population analyses and the electron density difference map. We further examined the noble gas matrix effects on the geometrical structure and vibrational frequencies of NiCO by performing density functional theory calculations for the Ng_{31}−NiCO (Ng = Ar, Ne, He) system. The present results will inspire the further experimental investigation on the complexes of noble gas and transition metal compounds generated in the matrix isolation experiments.

I. Introduction

In the matrix isolation infrared spectroscopy, vibrational spectra for weakly bound complexes can be recorded by utilizing the environmental matrix medium to eliminate the excess energy of the target species. This methodology is based on the nonreactivity of the matrix medium, and the frequency shifts from the gas phase are considered to be relatively small, typically less than 0.5%. According to the recent review on vibrational frequencies in binary unsaturated transition metal carbonyl compounds,[1] most spectroscopic data on the transition metal species have been determined using the matrix isolation technique. Noble gases are often used as the matrix medium because of their nonreactivity as a chemical species.

Although noble gases have difficulty making a chemical bond with other atoms, several compounds containing heavier noble gas elements, Xe or Kr, have been anticipated and prepared. On the other hand, the lighter noble gas elements, Ar, Ne, and He, are expected to be less reactive than the heavier ones because of the larger ionization energy, and actually, compounds containing Ar, Ne, or He have not been synthesized for a long time. The breakthrough came from theoretical consideration by Frenking and co-workers,[2] who predicted the existence of Ng−BeO (Ng = Ar, Ne, He) based on ab initio calculations. This prediction was realized, in part, by Thompson and Andrews, who detected the compounds, Ng−BeO (Ng = Xe, Kr, Ar), experimentally through pulsed-laser-ablation matrix isolation spectroscopy.[3] Räsänen and co-workers[4] found a new class of noble gas compounds, H−Ng−F (Ng = Xe, Kr), where HNg^+ and F^- bind with each other through a Coulomb attraction. In 2000, Räsänen et al. succeeded in the detection of H−Ar−F, which has brought an impact on the noble gas chemistry.[5] They verified that H−Ar−F is intrinsically stable owing to the significant ionic and covalent contributions to its bonding. Wong investigated the stability of a metastable helium compound, H−He−F, by ab initio calculations.[6] Takayanagi and Wada[7] performed three-dimensional wave packet calculations for H−He−F on the ab initio potential energy surface to discuss a lifetime of the lowest resonance state. As another class of noble gas complexes, Evans, Gerry, and co-workers detected a series of stable compounds of noble gas atom with a coinage metal monohalide, Ng−MX (Ng = Xe, Kr, Ar; M = Au, Ag, Cu; X = Br, Cl, F) and determined their geometrical structures by the microwave spectra.[8,9] Zhou and co-workers[10] performed matrix isolation infrared spectroscopic and theoretical studies for the first-row transition metal monoxides in solid noble gas matrices and found that late transition metal monoxides coordinate one noble gas atom in forming the Ng−MO complexes (Ng = Ar, Kr, Xe; M = Cr, Mn, Fe, Co, Ni), while the early transition metal monoxides, ScO, TiO, and VO, are not able to form similar noble gas atom complexes. Very recently we discussed the stability of the possible noble gas complexes of Ng−Pt−Ng′ and Ng−Pd−Ng′ (Ng, Ng′ = Xe, Kr, Ar) by highly accurate ab initio calculations.[11,12]

Along this line of research, we also reported a series of theoretical calculations on Ng−NiCO,[13,14] Ng−NiN_2,[14,15] and Ar−CoCO[14,16] in which an argon atom is shown to be bound to the transition metal compounds in a linear form with a binding energy of 5−10 kcal/mol. For NiCO, NiN_2, and CoCO, Manceron et al. measured vibrational frequencies using an argon matrix isolation technique and reported the bending frequency as 409.1 cm^{-1} (NiCO),[17] 357.0 cm^{-1} (NiN_2),[18] and 424.9 cm^{-1} (CoCO),[19] respectively. On the basis of density functional theory (DFT) calculations, we showed that the binding of Ar atom increases the bending frequency of each complex by ca. 10%, i.e., 361.1 to 403.5 cm^{-1} (Ar−NiCO), 308.5 to 354.8 cm^{-1} (Ar−NiN_2), and 373.0 to 422.6 cm^{-1} (Ar−CoCO). The intensity and isotopic shifts also showed that the experimental values are much closer to those calculated ones for Ar−NiCO, Ar−NiN_2, and Ar−CoCO than those for NiCO, NiN_2, and CoCO, respectively, and we suggested that the experimental spectra may be attributed to those of neutral argon complexes.

Following our report,[13] Tremblay and Manceron[20] reinvestigated the NiCO molecule in solid argon, neon, and mixed Ar/

* To whom correspondence should be addressed. E-mail: take@sci.hokudai.ac.jp.

10.1021/jp710792c CCC: $40.75
Published on Web 01/15/2008

TABLE 1: Calculated and Experimental Bond Lengths and Harmonic Frequencies for NiCO

		bond length (Å)		harmonic frequency (cm^{-1})		
level	basis set	r(Ni−C)	r(C−O)	ν(CO)	ν(NiCO)	ν(NiC)
MR-SDCI(+Q)	seg-QZP	1.6740	1.1545			
MR-SDCI(+Q)[a]	SK+aug-cc-pVTZ	1.6611	1.1574			
MR-SDCI(+Q)[b]	SK+aug-cc-pVTZ	1.650	1.159			
CCSD(T)	seg-QZP	1.6624	1.1569	2034	375	618
CCSD(T)[b]	SK+aug-cc-pVTZ	1.6419	1.1617	2017.3	401.7	633.3
CCSD(T)[c]	TZ-ANO	1.6755	1.1571	2028	372	600
CCSD(T)[c]	TZ-ANO/QZ	1.6732	1.1556			
B3LYP[b]	SK+aug-cc-pVTZ	1.663	1.149	2079.9	362.5	595.5
MPWPW91[b]	SK+aug-cc-pVTZ	1.654	1.164	2011.3	362.3	609.8
PW91PW91	seg-TZP	1.660	1.163	2026	364	620
experiment		1.669[d]	1.152[d]	2010.7[e]	363[f]	604[d]
		(1.6723)	(1.1512)			

[a] This calculation is based on the full-valence CASSCF wavefunction. [b] Reference 13. [c] Reference 33. [d] These numbers correspond to $r_m^{(2)}$, while those in parenthesis to r_0.[32] [e] This number corresponds to a fundamental frequency.[34] [f] Reference 35.

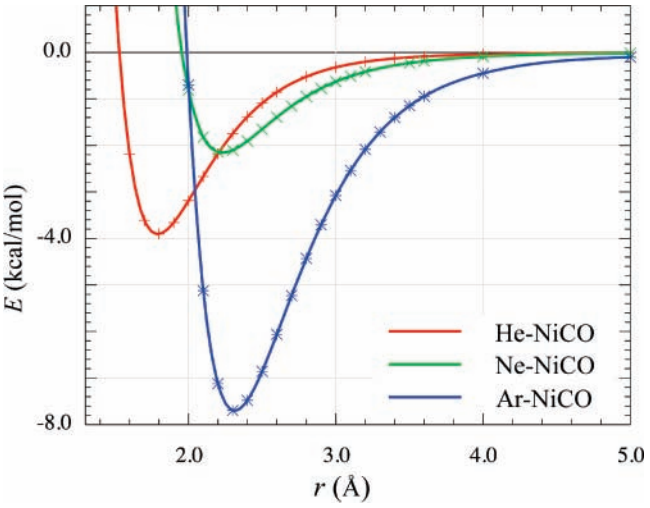

Figure 1. Potential energy curves for Ng−NiCO (Ng = Ar, Ne, He).

Ne matrices to attempt detecting a possible Ar−NiCO complex. It was reported that the absorptions observed in pure neon are weakly shifted from those in argon and that the relative isotopic shifts for the two noble gas atoms are the same. It was also found that adding progressively Ar to a Ne matrix demonstrates the existence of a progressive shift in the CO vibrational frequency of NiCO as the number of Ar atoms in the solvation shell increases progressively. On the basis of these results, they concluded that the species observed in solid argon should not be Ar−NiCO but NiCO.

In the present study we thoroughly reinvestigate the structures, binding energies, and vibrational frequencies for NiCO and Ng−NiCO (Ng = Ar, Ne, He) by the systematic theoretical calculations. The possibility of the formation of noble gas complexes is discussed in terms of an electron density difference map.

II. Computational Details

In the previous study for NiCO and Ng−NiCO (Ng = Ar, Ne, He),[13] we employed the complete active space self-consistent field (CASSCF), the multireference singles and doubles configuration interaction plus Davidson's correction (MR-SDCI(+Q)), the coupled-cluster singles and doubles including a perturbational estimate of triple excitations (CCSD(T)), and the DFT methods of B3LYP[21] and MPWPW91,[22] with the relativistic pseudopotentials of the Stuttgart/Köln group[23] (for Ne core) and related basis functions of (8s7p6d1f)/[6s5p3d1f] for 3s, 3p, 3d, and 4s electrons for Ni and the

TABLE 2: Bond Lengths (Å), Binding Energies (kcal/mol), and Harmonic Frequencies (cm^{-1}) for Ng−NiCO (Ng = Ar, Ne, He) Calculated by CCSD(T) with Basis Sets of seg-QZP and SK+aug-cc-pVTZ. Experimental Frequencies for NiCO by mmW and Matrix Isolation Method Also Given

bond length	r(Ni−C)	r(C−O)	r(Ng−Ni)	binding energy
		seg-QZP		
Ar−NiCO	1.675	1.157	2.314	7.70
Ne−NiCO	1.666	1.157	2.232	2.16
He−NiCO	1.674	1.156	1.791	3.91
		SK+aug-cc-pVTZ[a]		
Ar−NiCO	1.658	1.161	2.290	9.55
Ne−NiCO	1.649	1.161	2.160	3.71
He−NiCO	1.660	1.160	1.745	5.97

frequency	ν(CO)	ν(NiCO)	ν(NiC)	ν(NgNi)	ν(NgNiCO)
			seg-QZP		
Ar−NiCO	2045	423	609	188	72
Ne−NiCO	2051	411	618	154	64
He−NiCO	2054	424	609	421	129
			SK+aug-cc-pVTZ[a]		
Ar−NiCO	2029.0	439.6	613.1	193.8	60.7
Ne−NiCO	2032.3	432.6	621.5	176.2	66.5
He−NiCO	2037.7	435.5	609.9	479.0	113.3
			Experimental		
gas phase	2010.7[b]	363[c]	604[d]		
Ar matrix[e]	1994.5	409.1	591.1		
Ne matrix[f]	2006.7	398.9	592.9		

[a] Reference 13. [b] Reference 34. [c] Reference 35. [d] Reference 32. [e] Reference 17. [f] Reference 20.

Dunning's aug-cc-pVTZ basis set for other atoms (referred to as SK+aug-cc-pVTZ). In the present study, we apply the same methods, MR-SDCI(+Q) and CCSD(T), with more highly accurate all-electron basis sets, i.e., segmented basis sets of quadruple-ζ[24] plus correlation functions[25] (denoted as seg-QZP), to determine the equilibrium geometry of NiCO. In MR-SDCI calculations, the reference CASSCF wavefunction is determined with the full-valence active space (20 electrons in 14 orbitals), while the smaller active space (16 electrons in 11 orbitals) was used in the previous CASSCF-MR-SDCI calculations. After the comparison of the present and previous calculations with the experimental results for NiCO, we calculated the equilibrium geometry, binding energies, and harmonic frequencies for Ng−NiCO (Ng = Ar, Ne, He) by the CCSD(T)/seg-QZP method. The binding energy for Ng and NiCO was evaluated with a counterpoise correction to the basis set superposition error (BSSE). These calculations were carried out by the MOLPRO program.[26] We also performed natural population analyses to

TABLE 3: Bond Lengths (Å) and Harmonic and Fundamental Frequencies (cm^{-1}) for NiCO and Ng−NiCO Calculated by PW91PW91/seg-TZP

bond length	r(Ni−C)	r(C−O)	r(Ng−Ni)
Ar−NiCO	1.677	1.162	2.283
Ne−NiCO	1.665	1.162	2.180
He−NiCO	1.674	1.161	1.774

frequency	ν(CO)	ν(NiCO)	ν(NiC)	ν(NgNi)	ν(NgNiCO)
		Harmonic			
NiCO	2026	364	620		
Ar−NiCO	2023	409	600	185	52
Ne−NiCO	2025	400	616	167	42
He−NiCO	2030	413	604	434	126
		Fundamental			
NiCO	1995	359	610		
Ar−NiCO	1986	412	589	179	62
Ne−NiCO	1988	401	604	140	47
He−NiCO	1995	408	595	371	140
		Experimental			
gas phase	2010.7[a]	363[b]	604[c]		
Ar matrix[d]	1994.5	409.1	591.1		
Ne matrix[e]	2006.7	398.9	592.9		

[a] Reference 34. [b] Reference 35. [c] Reference 32. [d] Reference 17. [e] Reference 20.

give insights to the binding mechanism of Ng atom with NiCO at the CCSD/seg-QZP level, using the Gaussian03 program.[27]

To estimate the fundamental frequencies including the effect of the anharmonicity of the potential energy surface, we also carried out correlation-corrected vibrational self-consistent field (cc-VSCF) calculations[28] with the quartic-force-field potential energy surface[29] for NiCO and Ng−NiCO by the DFT method with PW91 exchange and correlation functionals (PW91PW91)[30] with the segmented basis sets of triple-ζ[24] plus correlation functions (seg-TZP)[25] using GAMESS.[31] We performed additional calculations for Ng_n−NiCO (Ng = Ar, Ne, He) by the MPWPW91/seg-TZP method to check the noble gas effects from the viewpoint of number of surrounding Ng atoms.

III. Results and Discussion

First we discuss the accuracy of our previous and present ab initio calculations by comparing the calculated results for NiCO. Table 1 summarizes the calculated and experimental bond lengths and harmonic frequencies for NiCO. Yamazaki and co-workers[32] determined the bond lengths at the zero-point vibrational energy level from the rotational spectrum for NiCO (numbers in parenthesis in Table 1) and then estimated the equilibrium bond lengths (r(NiC) = 1.669 Å and r(CO) = 1.152 Å in Table 1) that should be compared to the calculated bond lengths. They also estimated[32,35] harmonic frequencies for Ni−C−O bending and Ni−C stretching modes as 363 and 604 cm^{-1}, respectively. As to the C−O stretching mode, the fundamental frequency was reported as 2010.7 cm^{-1} from the vibrational spectrum for NiCO.[34] In MR-SDCI(+Q) calculations, we have improved the active space in the CASSCF wavefunctions and the basis sets from the previous ones.[13] The extension of the active space in the CASSCF wavefunction improved the Ni−C bond length from 1.650 to 1.6611 Å and the C−O bond length from 1.159 to 1.1574 Å, respectively. The improvement of the basis sets further works to make the calculated bond lengths closer to the experimental values, i.e., r(NiC) = 1.6740 Å and r(CO) = 1.1545 Å. As to CCSD(T) calculations, we also employed all-electron segmented QZP basis sets and obtained better results than the previous CCSD(T)/SK+aug-cc-pVTZ calculations (r(NiC) = 1.6419 → 1.6624 Å). Previous MR-SDCI(+Q) and CCSD(T) calculations estimated a shorter Ni−C bond length (by 0.02−0.03 Å) and a longer C−O bond length (by 0.01 Å), which should lead to the larger frequencies for Ni−C stretching and Ni−C−O bending modes and the smaller frequency for the C−O stretching mode. Schaefer et al.[33] performed systematic theoretical investigations for NiCO, and their best estimated Ni−C bond length was 1.6732 Å at the CCSD(T) level with the triple-ζ ANO (Ni) plus quadruple-ζ basis sets (C, O). Both our present and Schaefer et al.'s calculated bond lengths and harmonic frequencies are sufficiently converged to the experimental ones (the errors in bond lengths are 0.004−0.007 Å for Ni−C and 0.002−0.005 Å for C−O; the errors in harmonic frequencies are 9−12 cm^{-1} for the Ni−C−O bending mode and 4−14 cm^{-1} for the Ni−C stretching mode). Table 1 also shows results of DFT calculations by B3LYP, MPWPW91, and PW91PW91 methods. In spite of low computational costs, they show very good coincidence with the experimental values in both geometrical structures and harmonic frequencies.

Taking into account the higher accuracy of the CCSD(T)/seg-QZP calculations for NiCO compared to the previous CCSD(T)/SK+aug-cc-pVTZ calculations described above, we determined to apply the CCSD(T)/seg-QZP method to examine the structures, binding energies, and frequencies for the Ng−NiCO (Ng = Ar, Ne, He). It is noted that MR-SDCI(+Q) calculations on the Ng−NiCO system require too much computational cost. Figure 1 shows the counterpoise-corrected CCSD(T)/seg-QZP potential energy curves for Ng−NiCO as a function of r(Ng−Ni) where geometry of NiCO is fixed to that of the isolated one. It is clearly shown that each Ng atom is bound to NiCO with the binding energy that is much larger than the typical van der Waals interaction energy; Ng−NiCO can be referred to as "anomalously strong van der Waals cluster." It is noted that these complexes correspond to the global minimum on the potential energy surface. Interestingly, a He atom can be bound to NiCO with a larger binding energy than a Ne atom, with a shorter interatomic distance. This tendency is common to a series of Ng−BeO reported by Frenking and co-workers.[2] The binding energies for Ng and BeO were reported as 7.0 kcal/mol (Ar−BeO), 2.2 kcal/mol (Ne−BeO), and 3.1 kcal/mol (He−BeO) based on MP4(SDTQ)/6-311G-(2df,2pd) calculations, with corrections for zero-point vibrational energies and BSSE. These binding energies are very similar to those for Ng−NiCO. It was pointed out[2] that Ne and Ar possess (filled) p orbitals in their valence shells that are absent for He, and therefore repulsive p−π interactions involving the occupied 1π MOs of BeO are possible in Ar−BeO and Ne−BeO but not in He−BeO.

Table 2 shows equilibrium bond lengths, binding energies, and harmonic frequencies for Ng−NiCO calculated by the CCSD(T) method with several basis sets as well as the experimental values.[32] The CCSD(T)/seg-QZP method predicts that the counterpoise-corrected binding energy for Ng and NiCO is 7.70 kcal/mol (Ar−NiCO), 2.16 kcal/mol (Ne−NiCO), and 3.91 kcal/mol (He−NiCO). The previous CCSD(T)/SK+aug-cc-pVTZ calculations show larger binding energies since these energies were estimated with no correction for BSSE. As is the case for NiCO, the longer bond length leads to the smaller frequency of the corresponding vibrational mode, while the shorter bond length leads to the larger frequency. The comparison of Tables 1 and 2 indicates that, due to the interaction of Ng and NiCO, the Ni−C bond length becomes slightly longer while the CO bond length is almost unchanged.

TABLE 4: CCSD Natural Charge, Dipole Moment, and Change of Natural Orbital Population for Ng + NiCO → Ng−NiCO

	q(Ni)	q(C)	q(O)	q(Ng)	μ (Debye)		
NiCO	0.126	0.389	−0.515		3.508		
Ar−NiCO	−0.012	0.435	−0.510	0.087	4.103		
Ne−NiCO	0.065	0.418	−0.512	0.029	3.654		
He−NiCO	0.014	0.437	−0.504	0.053	3.336		
	Ng s	Ng p_σ	Ni 4s	Ni $3d_\sigma$	Ni $3d_\pi$	C 2s	C $2p_\pi$
Ar−NiCO	−0.029	−0.058	+0.114	−0.011	+0.028	−0.017	−0.022
Ne−NiCO	−0.011	−0.017	+0.076	−0.034	+0.016	−0.014	−0.012
He−NiCO	−0.052		+0.108	−0.037	+0.038	−0.018	−0.024

In Table 2, the matrix isolation experimental frequencies with Ar matrix[17] and Ne matrix[20] are also given in addition to the gas-phase experimental frequencies.[32,34,35] The main difference between the matrix isolation and gas-phase experiments is seen in the Ni−C−O bending frequency, although the gas-phase experimental value is not a fundamental but harmonic frequency for Ni−C−O bending and Ni−C stretching modes. The calculated harmonic frequencies also indicate that the binding of the Ng atom affects mainly the Ni−C−O bending frequency, which increases by ca. 10% (30−50 cm^{-1}). In the CCSD(T)/seg-QZP results, the shifts in the Ni−C−O bending frequency are calculated as 48 and 36 cm^{-1} for Ar−NiCO and Ne−NiCO, respectively, while the differences in Ni−C−O bending frequency between the gas-phase and matrix isolation experiments are 46 and 36 cm^{-1} for Ar and Ne matrices, respectively. The agreement in these frequency shifts suggests to us that the vibrational frequencies obtained from the matrix isolation experiments in refs 17 and 20 should be attributed to Ar−NiCO and Ne−NiCO, respectively. On the other hand, the C−O stretching frequency shows an increase by 11 cm^{-1} (Ar−NiCO) and by 17 cm^{-1} (Ne−NiCO) compared to that of NiCO in CCSD(T)/seg-QZP calculations, while it shows a decrease by 16 cm^{-1} (Ar−NiCO) and by 4 cm^{-1} (Ne−NiCO) in the experiment. However, it is noted that the relative rate in the increase or decrease of the C−O stretching frequency is only ∼0.8% and that the matrix effect on the Ni−C−O bending frequency (∼10%) is much larger. It is also noted that the calculated frequencies in Table 2 are harmonic ones, while the experimental frequencies are fundamental ones for the C−O stretching mode.

The rotational spectroscopy provides harmonic frequencies,[32,35] while the infrared spectroscopy provides fundamental frequencies[17,20,34] that are affected by the anharmonicity of the potential energy surface. In the previous study,[13] we discussed the anharmonicity effect on the Ni−C−O bending frequency by solving a one-dimensional vibrational Schrödinger equation for a Ni−C−O bending coordinate for NiCO and Ar−NiCO based on the CCSD(T)/SK+aug-cc-pVTZ potential energy curve. Per the results, the fundamental frequency for the Ni−C−O bending mode was estimated to be 418.6 and 454.3 cm^{-1} for NiCO and Ar−NiCO, respectively, which shows an increase of 15−17 cm^{-1} from the corresponding harmonic frequencies. Since these estimations do not take into account the anharmonicity of the potential couplings of normal coordinates, we have examined the anharmonicity effects on vibrational frequencies of NiCO and Ng−NiCO by performing cc-VSCF calculations based on PW91PW91 potential energy surface. Table 3 shows calculated bond lengths, harmonic frequencies, and fundamental frequencies. The comparison with the CCSD(T)/seg-QZP values in Tables 1 and 2 indicates that PW91PW91 can evaluate geometrical parameters and harmonic frequencies with high accuracy for NiCO and Ng−NiCO. At this computational level, the fundamental frequencies for the Ni−C−O bending mode were evaluated as 359, 412, and 401 cm^{-1} for NiCO, Ar−NiCO, and Ne−NiCO, respectively, where the anharmonicity effect to the Ni−C−O bending frequency is only 1−5 cm^{-1}. The corresponding experimental frequencies are 363, 409.1, and 398.9 cm^{-1}, respectively. The agreements of these numbers strongly support that Manceron et al.[20] detected the first neutral neon complex, Ne−NiCO, in the matrix isolation experiment. It is also shown that the anharmonicity effect works to decrease the C−O stretching frequency more largely in Ar−NiCO and Ne−NiCO than in NiCO. This effect is important to reproduce the order of the magnitude of the C−O stretching frequency for NiCO observed in the noble gas matrix.

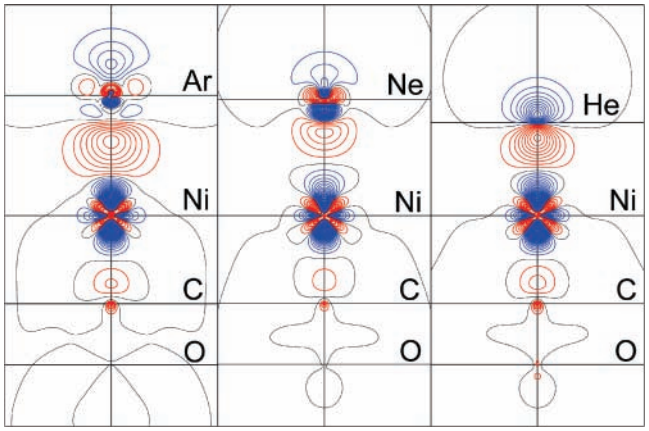

Figure 2. Contour map of electron density difference for Ng + NiCO → Ng−NiCO at the CCSD level.

Table 4 shows atomic natural charges q, dipole moments μ, and changes of atomic orbital populations due to the binding of Ng atom. NiCO has a dipole moment in the direction from a negatively charged O atom to a positively charged Ni atom. Atomic natural charges show that electron is transferred from Ng and C to Ni in Ng−NiCO, resulting in an almost zero charge on Ni. In Ar−NiCO, a part of the electron is transferred from Ar 3s and Ar $3p_\sigma$ to Ni 4s, which also acquires electrons from Ni $3d_\sigma$ and C 2s (forming a charge-transfer complex). It is also observed that a part of the electron is transferred from C $2p_\pi$ to Ni $3d_\pi$, indicating the decrease of π back donation from C to Ni. Actually the Ni−C bond in NiCO becomes slightly weak (the bond length increases) when Ar binds with NiCO. In Ne−NiCO, a similar electron transfer is observed although the transferred population is very small compared to the case of Ar−NiCO. In He−NiCO, however, a relatively large electron transfer is observed. This is because He has only K-shell electrons, and its atomic radius is so small that He comes closer to NiCO than Ne and Ar.

Figure 2 shows contour maps of the CCSD electron-density difference for Ng + NiCO → Ng−NiCO (Ng = Ar, Ne, He) where blue and red lines indicate the decrease and increase of electron density, respectively, and the step for each contour is 0.002. In Ar−NiCO, the electron density between Ar and Ni atoms increases due to the contribution from Ni 4s population.

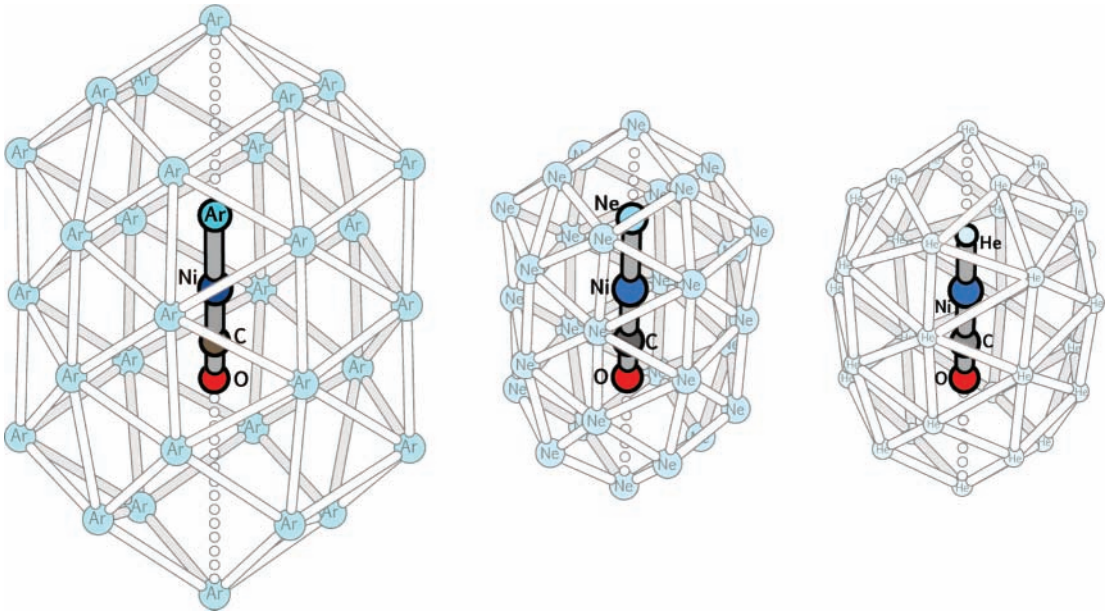

Figure 3. Optimized structures for Ng_{31}−NiCO (Ng = Ar, Ne, He).

TABLE 5: Bond Lengths (Å) and Harmonic Frequencies (cm^{-1}) for NiCO, Ng−NiCO, and Ng_{31}−NiCO Calculated by MPWPW91/seg-TZP

	bond length			harmonic frequency		
	r(Ni−C)	r(C−O)	r(Ng−Ni)	ν(CO)	ν(NiCO)	ν(NiC)
NiCO	1.662	1.163		2020	362	616
Ar−NiCO	1.679	1.163	2.293	2018	405	597
Ar_{31}−NiCO	1.678	1.163	2.296	2014	405	598
Ne−NiCO	1.666	1.163	2.236	2018	393	613
Ne_{31}−NiCO	1.665	1.164	2.260	2014	384	614
He−NiCO	1.675	1.162	1.805	2025	407	602
He_{31}−NiCO	1.674	1.162	1.806	2022	407	603

Since Ar 3s and Ar $3p_\sigma$ populations decrease simultaneously, the atomic dipole moment appears on the Ar atom, leading to the attraction between Ar and NiCO. It is noted that NiCO also has a dipole moment in the direction from O to Ni. On the Ni atom, the characteristic density difference appears due to the combination of negative contribution of $3d_\sigma$ and positive contribution of $3d_\pi$ where the change of the 4s population also contributes significantly. In the case of Ne−NiCO, the increase of the electron density between Ne and Ni atoms is much smaller than the one in Ar−NiCO, indicating the weaker attraction between Ne and NiCO. On the other hand, the increase in the middle region of He and NiCO seems close to the case of Ar−NiCO. This feature can be related to the small interatomic distance between He and Ni atoms.

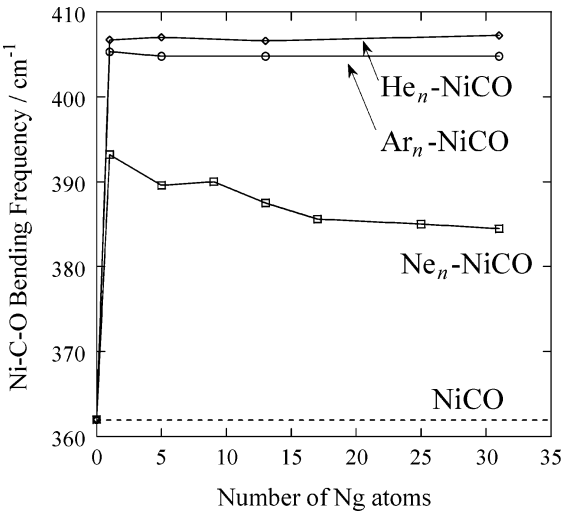

Figure 4. Variation of Ni−C−O bending frequencies for Ng_n−NiCO (Ng = Ar, Ne, He) as a function of the number of Ng atoms.

We also performed additional MPWPW91/seg-TZP calculations for Ng_n−NiCO (Ng = Ar, Ne, He) to examine the interaction of NiCO with surrounding Ng atoms in the noble gas matrix. The MPWPW91 method was designed[21] to reproduce a van der Waals interaction by modifying the PW91PW91 method, and so it is expected that MPWPW91 gives a reasonable description for Ng−Ng interactions. To make a modeling for NiCO in bulk noble gases, the noble gas cluster consisting of 33 Ng atoms is prepared, and the central two Ng atoms are replaced with NiCO where positions of Ng atoms are taken from the crystal data. Then, geometry optimizations were performed for Ng_{31}−NiCO (Ng = Ar, Ne, He) with no geometrical restrictions, and the following normal-mode analyses were carried out. Figure 3 shows the optimized structures for each system. The size of the cluster systems is related to the van der Waals radius of each noble gas atom. As shown here, one Ng atom approaches Ni in NiCO, while the other Ng atoms do not approach NiCO. The structures in Figure 3 indicate that NiCO in bulk noble gases can be easily transformed to Ng−NiCO. Table 5 shows bond lengths and harmonic frequencies for NiCO, Ng−NiCO, and Ng_{31}−NiCO (Ng = Ar, Ne, He) calculated by the MPWPW91/seg-TZP method. According to the comparison of the Ng−Ni bond length and Ni−C−O bending frequency between Ng−NiCO and Ng_{31}−NiCO, only the Ne_{31}−NiCO system shows a relatively large deviation, i.e., Ne−Ni interatomic distance increases by 0.024 Å and the Ni−C−O bending

frequency decreases by 9 cm^{-1}. To examine the dependency of the Ni−C−O bending frequency on the number of Ng atoms, we carried out a series of calculations for several sizes of clusters of Ng_n−NiCO. Variations of the Ni−C−O bending frequency are shown in Figure 4. As shown here, the first one noble gas atom works significantly to increase the bending frequency by ca. 10% in all cases. The succeeding Ng atoms do not change the bending frequency in Ar_n and He_n clusters, while in the Ne_n cluster, the bending frequency continues to decrease as the number of surrounding Ng atoms increases and seems to converge to 385 cm^{-1}. This behavior should be related to the weakest interaction between Ne and NiCO among Ng−NiCO. In spite of this decrease, however, the effect from the first Ne atom is significantly large compared to the van der Waals interaction, and thus Ne−NiCO can be regarded as the charge-transfer complex.

IV. Concluding Remarks

We re-examined geometrical structures, binding energies, and vibrational frequencies for NiCO and Ng−NiCO by highly accurate ab initio CCSD(T) methods with the segmented QZP basis sets. The present results have brought us an idea that the origin of the matrix shift is, in some cases, attributed to a formation of the noble gas charge-transfer complex in the matrix environment. It will inspire further experimental investigation in the field of noble gas chemistry. It should be noted that the detailed study by Manceron et al. revealed the existence of Ne−NiCO, which is the first ever experimental report on a stable neutral neon complex.

Acknowledgment. We acknowledge Dr. E. Okabayashi for valuable discussions. Y. T. gives thanks to the Japan Society for the Promotion of Science for Research Fellowships for Young Scientist.

References and Notes

(1) Zhou, M.; Andrews, L.; Bauschlicher, C. W., Jr. *Chem. Rev.* **2001**, *101*, 1931.
(2) Frenking, G.; Koch, W.; Gauss, J.; Cremer, D. *J. Am. Chem. Soc.* **1988**, *110*, 8007.
(3) Thompson, C. A.; Andrews, L. *J. Am. Chem. Soc.* **1994**, *116*, 423.
(4) Pettersson, M.; Lundell, J.; Räsänen, M. *J. Chem. Phys.* **1995**, *102*, 6423.
(5) Khriachtchev, L.; Pettersson, M.; Runeberg, N.; Lundell, J.; Räsänen, M. *Nature* **2001**, *406*, 874.
(6) Wong, M. W. *J. Am. Chem. Soc.* **2000**, *122*, 6289.
(7) Takayanagi, T.; Wada, A. *Chem. Phys. Lett.* **2002**, *352*, 91.
(8) Evans, C. J.; Gerry, M. C. L. *J. Chem. Phys.* **2000**, *112*, 1321.
(9) Evans, C. J.; Gerry, M. C. L. *J. Chem. Phys.* **2000**, *112*, 9363.
(10) Zhao, Y. Y.; Gong, Y.; Zhou, M. F. *J. Phys. Chem. A* **2006**, *110*, 10777.
(11) Ono, Y.; Taketsugu, T.; Noro, T. *J. Chem. Phys.* **2005**, *123*, 204321.
(12) Taketsugu, Y.; Taketsugu, T.; Noro, T. *J. Chem. Phys.* **2006**, *125*, 154308.
(13) Ono, Y.; Taketsugu, T. *Chem. Phys. Lett.* **2004**, *385*, 85.
(14) Ono, Y.; Taketsugu, T. *Chem. Monthly* **2005**, *136*, 1087.
(15) Ono, Y.; Taketsugu, T. *J. Chem. Phys.* **2004**, *120*, 6035.
(16) Ono, Y.; Taketsugu, T. *J. Phys. Chem. A* **2004**, *108*, 5464.
(17) Joly, H. A.; Manceron, L. *Chem. Phys.* **1998**, *226*, 61.
(18) Manceron, L.; Alikhani, M. E.; Joly, H. A. *Chem. Phys.* **1998**, *228*, 73.
(19) Tremblay, B.; Alikhani, M. E.; Manceron, L. *J. Phys. Chem. A* **2001**, *105*, 11388.
(20) Tremblay, B.; Manceron, L. *Chem. Phys. Lett.* **2006**, *429*, 464.
(21) Becke, A. D. *J. Chem. Phys.* **1993**, *98*, 5648.
(22) Adamo, C.; and Barone, V. *J. Chem. Phys.* **1998**, *108*, 664.
(23) Dolg, M.; Wedig, U.; Stoll, H.; Preuss, H. *J. Chem. Phys. 86*, 866.
(24) Tatewaki, H.; Koga, T. *J. Chem. Phys.* **1996**, *104*, 8493.
(25) Noro, T.; Sekiya, M.; Koga, T. *Theor. Chem. Acc.* **1997**, *98*, 25.
(26) Werner, H.-J.; Knowles, P. J.; Lindh, R.; Manby, F. R.; Schutz, M. *MOLPRO*, version 2006.1; http://www.molpro.net.
(27) Frisch, M. J.; Trucks, G. W.; Schlegel, H. B.; Scuseria, G. E.; Robb, M. A.; Cheeseman, J. R.; Montgomery, J. A., Jr.,; Vreven, T.; Kudin, K. N.; Burant, J. C.; Millam, J. M.; Iyengar, S. S.; Tomasi, J.; Barone, V.; Mennucci, B.; Cossi, M.; Scalmani, G.; Rega, N.; Petersson, G. A.; Nakatsuji, H.; Hada, M.; Ehara, M.; Toyota, K.; Fukuda, R.; Hasegawa, J.; Ishida, M.; Nakajima, T.; Honda, Y.; Kitao, O.; Nakai, H.; Klene, M.; Li, X.; Knox, J. E.; Hratchian, H. P.; Cross, J. B.; Bakken, V.; Adamo, C.; Jaramillo, J.; Gomperts, R.; Stratmann, R. E.; Yazyev, O.; Austin, A. J.; Cammi, R.; Pomelli, C.; Ochterski, J. W.; Ayala, P. Y.; Morokuma, K.; Voth, G. A.; Salvador, P.; Dannenberg, J. J.; Zakrzewski, V. G.; Dapprich, S.; Daniels, A. D.; Strain, M. C.; Farkas, O.; Malick, D. K.; Rabuck, A. D.; Raghavachari, K.; Foresman, J. B.; Ortiz, J. V.; Cui, Q.; Baboul, A. G.; Clifford, S.; Cioslowski, J.; Stefanov, B. B.; Liu, G.; Liashenko, A.; Piskorz, P.; Komaromi, I.; Martin, R. L.; Fox, D. J.; Keith, T.; Al-Laham, M. A.; Peng, C. Y.; Nanayakkara, A.; Challacombe, M.; Gill, P. M. W.; Johnson, B.; Chen, W.; Wong, M. W.; Gonzalez, C.; Pople, J. A. *Gaussian 03*, revision C.02; Gaussian, Inc., Wallingford CT, 2004.
(28) Chaban, G. M.; Jung, J. O.; Gerber, R. B. *J. Chem. Phys.* **1999**, *111*, 1823.
(29) Yagi, K.; Hirao, K.; Taketsugu, T.; Schmidt, M. W.; Gordon, M. S. *J. Chem. Phys.* **2004**, *121*, 1383.
(30) Perdew, J. P.; Chevray, J. A.; Vosko, S. H.; Jackson, K. A.; Pederson, M. R.; Singh, D. J.; Fiolhais, C. *Phys. Rev. B* **1992**, *46*, 6671.
(31) Schmidt, M. W.; Baldridge, K. K.; Boatz, J. A.; Elbert, S. T.; Gordon, M. S.; Jensen, J. H.; Koseki, S.; Matsunaga, N.; Nguyen, K. A.; Su, S.; Windus, T. L.; Dupuis, M.; Montgomery, J. A. *J. Comput. Chem.* **1993**, *14*, 1347.
(32) Yamazaki, E.; Okabayashi, T.; Tanimoto, M. *J. Am. Chem. Soc.* **2004**, *126*, 1028.
(33) Homy, L.; Paul, A.; Yamaguchi, Y.; Schaefer, H. F., III. *J. Chem. Phys.* **2004**, *121*, 1412.
(34) Martinez, A.; Morse, M. D. *J. Chem. Phys.* **2006**, *124*, 124316.
(35) Yamamoto, T.; Okabayashi, E.; Okabayashi, T.; Tanimoto, M. *The 1st Symposium of Japan Society for Molecular Science*, abstract 1P104, 2007.